The Plant Journal (2004) **40**, 968–978 doi: 10.1111/j.1365-313X.2004.02264.x

Mutations in *PMR5* result in powdery mildew resistance and altered cell wall composition

John P. Vogel[1,*], Theodore K. Raab[2], Chris R. Somerville[2,3] and Shauna C. Somerville[2]
[1]*USDA Western Regional Research Center, Albany, CA 94710, USA,*
[2]*Department of Plant Biology, Carnegie Institution, Stanford, CA 94305, USA, and*
[3]*Department of Biological Sciences, Stanford University, Stanford, CA 94305, USA*

Received 6 August 2004; revised 16 September 2004; accepted 17 September 2004.
[*]For correspondence (fax +510 559 5818; e-mail jvogel@pw.usda.gov).

Summary

Powdery mildews and other obligate biotrophic pathogens are highly adapted to their hosts and often show limited host ranges. One facet of such host specialization is likely to be penetration of the host cell wall, a major barrier to infection. A mutation in the *pmr5* gene rendered Arabidopsis resistant to the powdery mildew species *Erysiphe cichoracearum* and *Erysiphe orontii*, but not to the unrelated pathogens *Pseudomonas syringae* or *Peronospora parasitica*. *PMR5* belongs to a large family of plant-specific genes of unknown function. *pmr5*-mediated resistance did not require signaling through either the salicylic acid or jasmonic acid/ethylene defense pathways, suggesting resistance in this mutant may be due either to the loss of a susceptibility factor or to the activation of a novel form of defense. Based on Fourier transform infrared analysis, the *pmr5* cell walls were enriched in pectin and exhibited a reduced degree of pectin modification relative to wild-type cell walls. In addition, the mutant had smaller cells, suggesting a defect in cell expansion. A double mutant with *pmr6* (defective in a glycosylphosphatidylinositol-anchored pectate lyase-like gene) exhibited a strong increase in total uronic acid content and a more severe reduction in size, relative to the single mutants, suggesting that the two genes affect pectin composition, either directly or indirectly, via different mechanisms. These two mutants highlight the importance of the host cell wall in plant–microbe interactions.

Keywords: Arabidopsis, cell wall, disease susceptibility, disease resistance, pectin, powdery mildew.

Introduction

Plant pathogens have evolved a variety of strategies for extracting nutrients from their hosts. At one extreme lie the necrotrophic pathogens that actively kill host tissues and then proliferate in the wreckage (e.g. *Botrytis* spp.). At the other extreme lie obligate biotrophic pathogens that can grow only on living plant tissues. Biotrophic pathogens have evolved the ability to extract nutrients from their hosts without killing them. In addition, these pathogens must evade or suppress host defenses until their life cycle is complete. Powdery mildew fungi are excellent examples of obligate biotrophic pathogens. Indeed, the growth requirements of these pathogens are so exacting that they have never been cultured on artificial media. Given the intimacy of the relationship between obligate biotrophs and their hosts, it seems possible that some host genes would be required for pathogen growth. If such host susceptibility genes were mutated, assuming the genes were not redundant or essential for host survival, then pathogen growth would be reduced. Phenotypically such mutants would appear disease-resistant (Panstruga, 2003; Schulze-Lefert and Vogel, 2000). Based on this reasoning, we developed a screen to recover loss-of-susceptibility to mutants of Arabidopsis, the *powdery mildew-resistant* (*pmr*) mutants (Vogel and Somerville, 2000; Vogel *et al.*, 2002). Twenty-six mutants in six complementation groups, *pmr1–pmr6*, were isolated. Two of the *PMR* genes have been cloned. *PMR4* (=*CALS12*, =*GLS5*) encodes a wound and pathogen-associated callose synthase, and *PMR6* codes for a pectate-lyase-like protein (Nishimura *et al.*, 2003; Vogel *et al.*, 2002). The diverse nature of the *PMR* genes cloned to date highlights the range of plant processes that contribute to powdery mildew disease development.

Due to the general nature of this screen, gain-of-resistance mutants were also expected. Introducing mutations or transgenes that block flux through known defense pathways into the *pmr* mutants is one valuable method for distinguishing loss-of-susceptibility from gain-of-resistance mutants (Glazebrook, 2001). *pmr4* resistance was dependent on a functional salicylic acid (SA) signal transduction pathway suggesting that this mutant was a gain-of-resistance mutant (Nishimura *et al.*, 2003). However, similar double mutant experiments demonstrated that *pmr6*-mediated resistance did not require either the SA or the jasmonate (JA)/ethylene pathways (Vogel *et al.*, 2002). Thus, PMR6 is either required for susceptibility or *pmr6* mutations activate an undescribed defense pathway, suggesting PMR6 is a novel host component of plant–microbe interactions.

Cloning of the *PMR6* gene revealed that it was a member of a large family of cell wall-degrading pectate lyases (Vogel *et al.*, 2002). However, PMR6 differs from other pectate lyases in the Arabidopsis genome by a novel C-terminal domain with a glycosylphosphatidylinositol anchor motif. Fourier transform infrared spectroscopy (FTIR) analysis revealed that cell walls from uninfected *pmr6* plants were spectroscopically distinct from wild-type cell walls. Although the spectroscopic differences could not be unambiguously deconvoluted, they were consistent with increased pectin content, reduced pectin esterification and a change in the hydrogen-bonding environment of cellulose in the mutant relative to wild-type cell walls. Cross-linking of pectin components determines the porosity of the cell wall and the charged sugar residues in pectin components determine the ionic environment of the wall, both features that could impact pathogen interactions with its host (Vincken *et al.*, 2003). As pectin is thought to play a role in the complex process of cell wall expansion, the altered pectin content of *pmr6* cell walls may contribute to the reduced size of this mutant.

In the same screen for powdery mildew-resistant mutants that gave rise to *pmr1* to *pmr4* and *pmr6*, we identified another mutant, *pmr5*, which was morphologically very similar to and had the same disease resistance phenotype as *pmr6*, but belonged to a different complementation group. Here we describe the cloning and characterization of *PMR5*.

Results

Mutant isolation and fungal growth

The *pmr5* mutant was identified as being highly resistant to powdery mildew (Vogel and Somerville, 2000). Crosses between *pmr5* and the other *pmr* loci indicated that *pmr5* defined a new complementation group. An F_2 population from a *pmr5* × Col cross segregated 74 susceptible:22 resistant plants, which fit a 3:1 segregation ($\chi^2 = 0.22$, $P = 0.64$) expected of a single, recessive Mendelian locus.

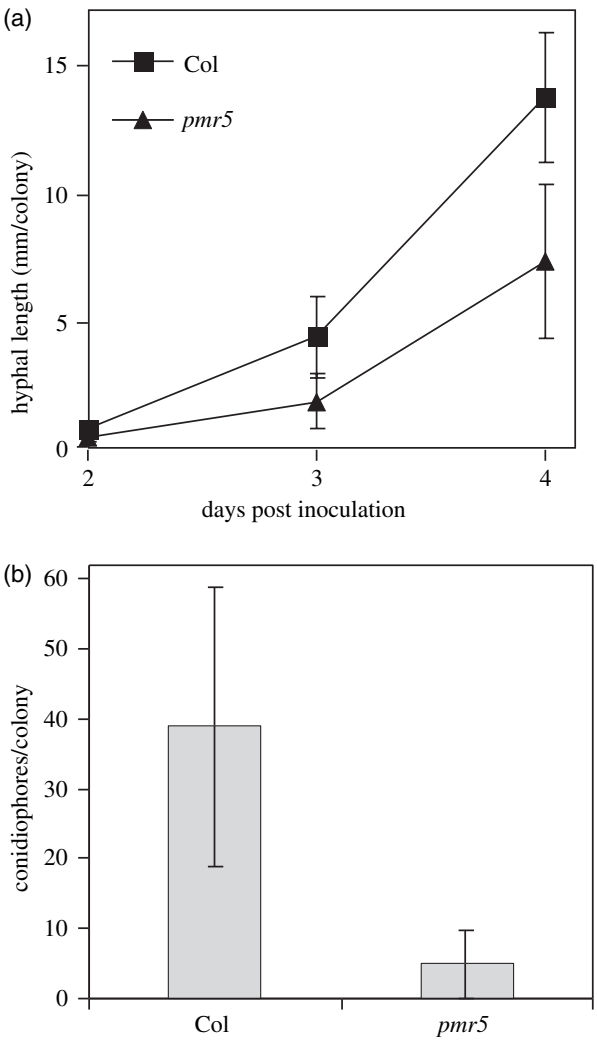

Figure 1. Quantification of *Erysiphe cichoracearum* growth.
(a) Hyphal length per colony.
(b) Conidiophores per colony at 6 dpi.
Mean ± SD based on 15 colonies are presented in both (a) and (b).

To quantify powdery mildew resistance, hyphal growth and asexual reproduction was measured (Vogel and Somerville, 2000). From 2 days post-inoculation (dpi) and beyond, hyphal growth was significantly (*t*-test, $P < 0.01$) lower on *pmr5* plants than on wild type (Figure 1a). Likewise, conidiation was significantly (*t*-test, $P < 10^{-6}$) reduced on *pmr5* (Figure 1b). These results indicate that *pmr5* resistance was not due to a block at a specific stage of fungal growth. Rather, the fungus simply failed to thrive on *pmr5* plants.

Contribution of known defenses

To determine the activation state of the SA and JA/ethylene pathways in the *pmr5* mutant, we measured the steady-state

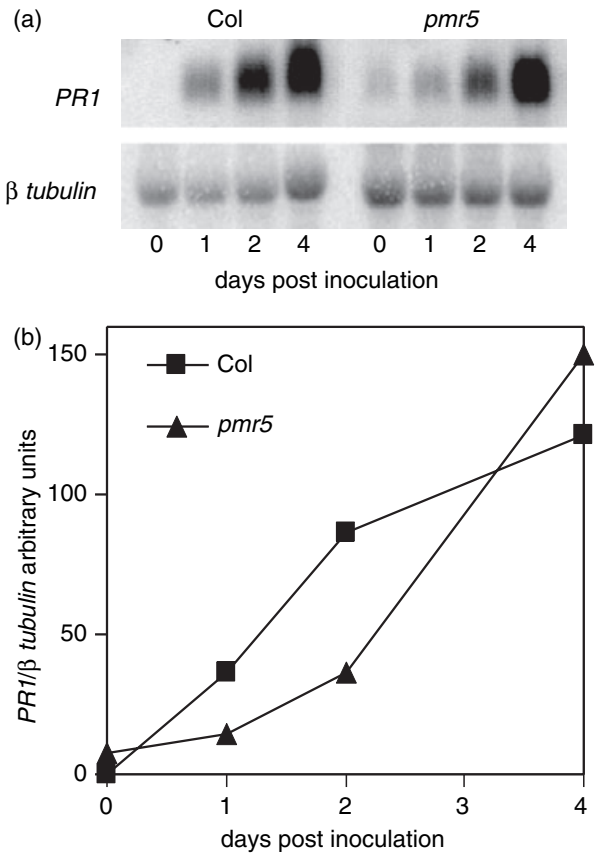

Figure 2. Time course of *PR1* mRNA accumulation following inoculation with powdery mildew.
(a) RNA gel blot probed with *PR1* and β-tubulin.
(b) *PR1* intensity from A was normalized to β-tubulin intensity and plotted versus dpi. Similar trends were observed in two other experiments using slightly different time points.

levels of *PR1* and *PDF1.2* mRNAs. For the 4 days after inoculation, *PR1* mRNA levels in *pmr5* plants were approximately the same or modestly reduced relative to wild type (Figure 2). Thus, *pmr5* resistance was not mediated by a hyper-activation of the SA pathway. However, we observed that *pmr5* plants constitutively expressed a low and variable amount of *PR1*. To determine whether this low-level constitutive activation of the SA pathway was responsible for the resistance, we introduced the *npr1-1* mutation and the *NahG* transgene into the *pmr5* background with sexual crosses. The *NahG* transgene encodes a salicylate hydroxylase that degrades SA to catechol and has been widely used to block SA signaling (Lawton *et al.*, 1995). *pmr5 NahG* plants were still resistant to powdery mildew (Figure 3) despite no longer expressing detectable levels of *PR1* mRNA (not shown). *NPR1* is a downstream component in the SA signal transduction pathway (Cao *et al.*, 1994). Similar to *NahG*, the *npr1* mutation blocks signaling through the SA pathway. Consistent with the *pmr5 NahG* results, *pmr5 npr1-1* plants were resistant to powdery mildew. Importantly, as *NPR1* is also required for the activation of induced systemic resistance, this pathway cannot be responsible for *pmr5* resistance.

To evaluate the contribution of the JA/ethylene pathway to *pmr5* resistance, we determined the steady-state level of *PDF1.2* mRNA after inoculation and determined the effect of mutations that block ethylene or JA signaling on *pmr5* resistance (Glazebrook, 2001; Penninckx *et al.*, 1996). Unlike *PR1*, no induction of *PDF1.2* was observed in wild type or *pmr5* after inoculation (not shown). Not surprisingly, mutations that block ethylene signaling (*ein2-1*; Alonso *et al.*, 1999) or JA signaling (*coi1*; Xie *et al.*, 1998) had no effect on *pmr5*-mediated resistance (Figure 3). Thus, *pmr5*-mediated resistance does not require signaling through the SA or JA/ethylene pathways leaving open the possibility that PMR5 is required for fungal growth or that the *pmr5* mutation leads to the activation of a novel defense mechanism.

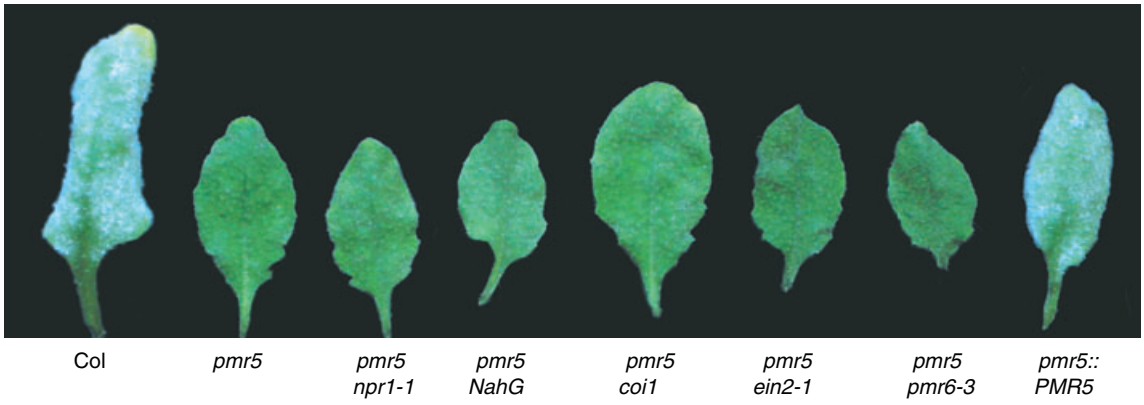

Figure 3. Effects of various mutations on the *pmr5* phenotype.
Plants were inoculated 11 days prior to being photographed. Note the lack of fungal growth on lines homozygous for the *pmr5* mutation, irrespective of other mutations (*npr1-1*, *coi1*, *ein2-1*) and ectopic expression of *NahG*, which alter defense signaling. Also note that transgenic complementation of the *pmr5* mutation with the wild-type gene (i.e. *pmr5:PMR5)* restored susceptibility. Plants were 25 days old when photographed. Leaves displaying typical reactions are shown.

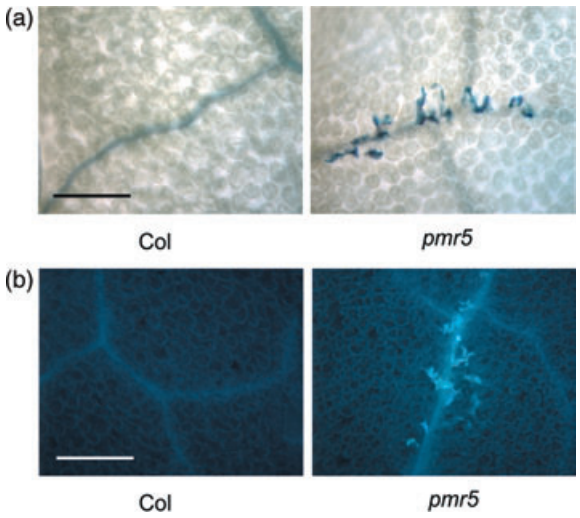

Figure 4. Microlesion phenotype.
(a) Uninfected leaves stained with trypan blue. Dead cells stain dark blue. Note that individual mesophyll cells along some veins are stained in *pmr5*. Veins appear as dark lines.
(b) The accumulation of autofluorescent compounds, as indicated by bright blue spots, follows the same pattern as dead cells in *pmr5*. Veins appear as blue lines. Bars in (a) and (b) are 200 μm. Leaves were sampled from 3-week-old plants.

Cell death is thought to play a key role in the resistance mediated by most resistance genes and by some mutations conferring resistance to various pathogens. To determine whether *pmr5*-mediated resistance correlated with cell death, we used trypan blue staining to identify dead cells in *pmr5* and wild-type leaves. At 1 dpi, we did not observe any dead cells beneath fungal colonies. At 5 dpi, we observed dead cells beneath a small percentage of colonies on both wild type and *pmr5* leaves. Importantly, we observed many dead or dying fungal colonies (shrunken, detached hyphae) on top of living *pmr5* cells. Thus, cell death is not required for *pmr5*-mediated resistance. While we did not observe increased cell death after infection, we did notice a variable number of individual dead mesophyll cells on *pmr5* leaves (Figure 4a). These dead cells were typically found along the veins on the outermost edge on some of the oldest leaves. The dead cells were also autofluorescent suggesting that phenolic compounds had been cross-linked into the cell wall (Figure 4b). These microlesions did not increase after inoculation. All *pmr5* leaves were highly resistant to powdery mildew, while only some of the oldest leaves contained microlesions. Thus, *pmr5* resistance did not require these microlesions. We view the microlesions as a pleiotropic effect of the *pmr5* mutation.

Plants reinforce the cell wall at sites of attempted fungal penetration by forming papillae. As resistance in some barley cultivars and the *mlo* mutant correlates with an enhanced papillae response, we examined *pmr5* papillae. Papillae were visualized by staining with aniline blue, which renders callose, a major component of the papillae, fluorescent. No differences between wild type and *pmr5* were observed at 1, 2, or 3 dpi (data not shown).

Table 1 Rosette diameter

Genotype	Mean rosette diameter (mm)	SD	*n*
Col	71	5.0	41
pmr5	38	3.0	47
pmr6-3	48	6.0	43
pmr5 pmr6-3	23	2.6	37

All mean values were significantly different based on ANOVA ($P < 10^{-99}$) and *t*-tests ($P < 10^{-15}$).

Other pathogens

To determine the specificity of *pmr5*-mediated resistance, we challenged *pmr5* plants with the bacterial pathogen *Pseudomonas syringae* pv tomato DC3000 (Whalen *et al.*, 1991), the oomycete pathogen *Peronospora parasitica* EMCO5 (Dangl *et al.*, 1992) and another powdery mildew species, *Erysiphe orontii* MGH1 (Plotnikova *et al.*, 1998). After inoculation with several concentrations (10^6–10^8) of *P. syringae* pv tomato, symptoms on *pmr5* plants were indistinguishable from wild type (data not shown). To determine whether the symptoms were indicative of pathogen growth, a growth curve was constructed by grinding leaf disks and plating dilutions on selective media. The growth curves for *pmr5* and wild type were essentially identical (not shown). Thus, *pmr5* was fully susceptible to *P. syringae* pv tomato.

We challenged *pmr5* with *P. parasitica*, an unrelated obligate biotrophic pathogen. *pmr5* (67 ± 14) was equally susceptible to *P. parasitica* as Col (64 ± 16) as measured by sporangiophore production (values are mean of sporangiophores per seedling ±SD, based on 20 seedlings). The entire experiment was repeated once with similar results.

pmr5 was also challenged with *E. orontii* to determine whether the resistance was specific to *E. cichoracearum*. Nine of nine *pmr5* plants from five independent experiments showed no *E. orontii* growth at 7 dpi, while Col controls showed extensive *E. orontii* growth. Thus, *pmr5*-mediated resistance is effective against isolates from two different species of powdery mildew.

Morphology

Under standard growth conditions, the size of *pmr5* plants differed from wild type, indicating that *PMR5* plays a role in plant growth and development. The largest diameters of *pmr5* rosettes (40 ± 3.7 mm; 19 rosettes) were smaller than those of Col (70 ± 3.2 mm; 18 rosettes). The area of representative epidermal cells was 4600 ± 1600 μm^2 $cell^{-1}$ for Col

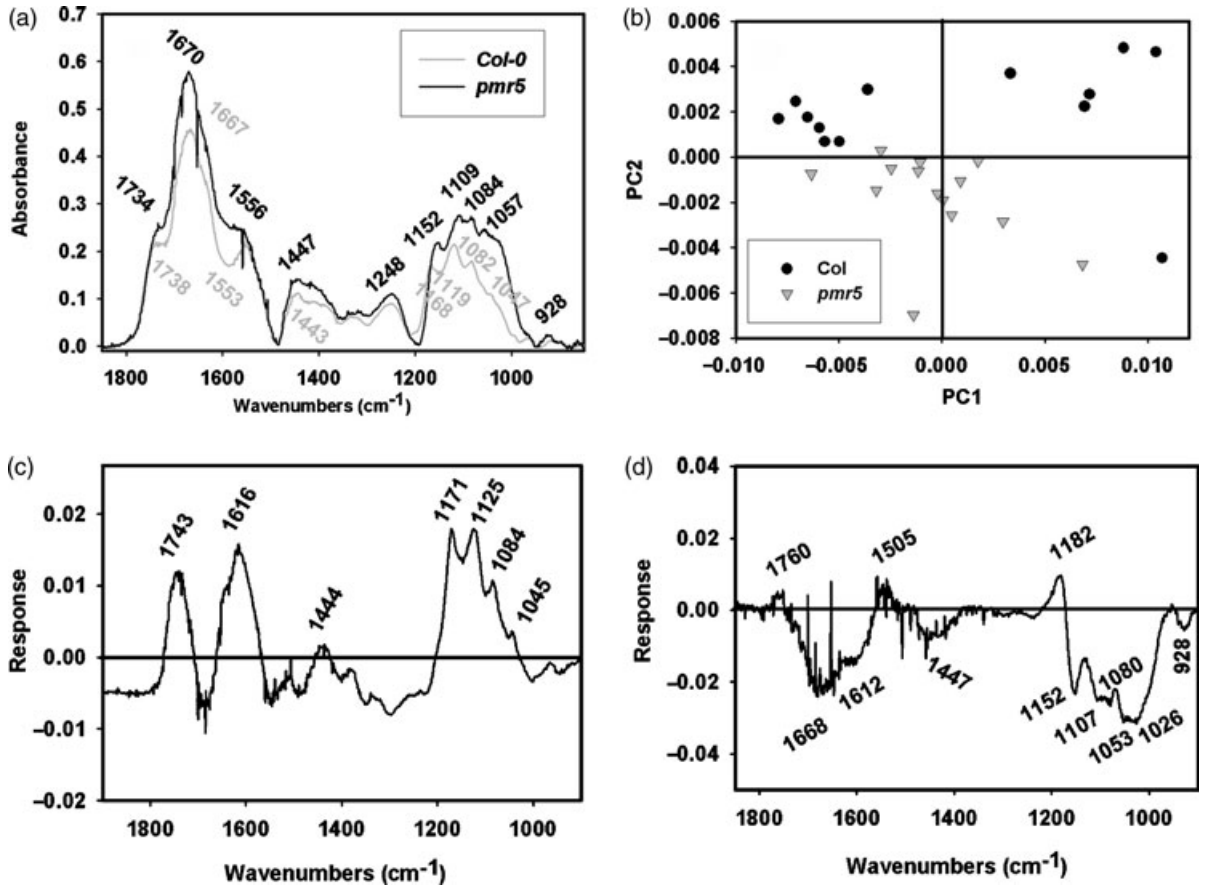

Figure 5. FTIR analysis of *pmr5* and Col cell walls.
(a) Averaged mid-infrared absorption spectra from the adaxial leaf surface of Col (lower, gray curve; $n = 12$) and *pmr5* (upper, black curve; $n = 14$). In the polysaccharide-rich absorption region from 1200 to 950 cm^{-1} of *pmr5* cell walls, the highest energy cellulose and xyloglucan-related absorption was shifted down by about 8–14 cm^{-1}, and higher overall absorption from 1080 to 980 cm^{-1} was observed compared with wild type.
(b) Biplot showing the separation of Col and *pmr5* spectra generated by the covariance-matrix approach for principal component analysis. Note that Col and *pmr5* form two distinct populations.
(c, d) First and second principal components of the covariance-matrix separation of the data sets summarized in (a). (c) The first principal component eigenvector. (d) The second principal component eigenvector has features attributable to either xyloglucan (Kacurakova *et al.*, 2000) or pectins (Coimbra *et al.*, 1998; Synytsya *et al.*, 2003; Wilson *et al.*, 2000) at 1152 and 1107 cm^{-1} (Coimbra *et al.*, 1998; Synytsya *et al.*, 2003; Wilson *et al.*, 2000). A 1080 cm^{-1} feature assignable to arabinogalactan-rich pectin (Kacurakova *et al.*, 2000) and pectin features at 1053 and 1026 cm^{-1} (Wellner *et al.*, 1998) suggest an enrichment in unesterified pectin in *pmr5* relative to Col. The amide-I absorption peak at 1668 cm^{-1} may reflect a higher protein content in the smaller *pmr5* leaves (Pelton and McLean, 2000). The broad, poorly resolved shoulder centered at 1612 cm^{-1} encompasses spectral features for carboxylate groups from pectin, although cellulose also absorbs at this energy, perhaps consistent with the cellulose anomeric band or pectin *O*-acetyl band at 928 cm^{-1} (Synytsya *et al.*, 2003).

(69 cells from four leaves) and 1600 ± 640 μm^2 $cell^{-1}$ for *pmr5* (85 cells from four leaves) (values given are mean ± SD). Thus, *pmr5* rosettes were 0.57 times the diameter of wild-type rosettes, and *pmr5* epidermal cells were 0.35 times the area of wild-type epidermal cells. By comparing the square of the rosette diameter ratio ($0.57^2 = 0.32$) with the ratio of the epidermal cell area (0.35), we conclude that the reduction in the size of *pmr5* rosettes was primarily due to a decrease in cell expansion. Like *pmr6* leaves, *pmr5* leaves were shorter, rounder, and cupped slightly upward when compared with wild-type leaves, which curled down (Figure 3).

Given the similarity of *pmr5* and *pmr6* phenotypes, we tested whether these two genes act additively to influence size. Both *pmr5* and the *pmr5 pmr6-3* double mutant were significantly smaller than *pmr6-3* (Table 1). Importantly, *pmr5 pmr6-3* rosettes were smaller than *pmr5* rosettes indicating that the mutations were not epistatic.

Cell wall analysis

We examined the composition of *pmr5* cell walls using FTIR spectroscopy as was the case for *pmr6* (Vogel *et al.*, 2002). Visual inspection of the spectra from *pmr5* revealed greater absorbance in the 1730–1740 cm^{-1} shoulder region attributed to pectin esters, indicating that *pmr5* cell walls may contain more pectin than wild type (Figure 5a) (Fillipov, 1972; Synytsya *et al.*, 2003). The relative widths of the

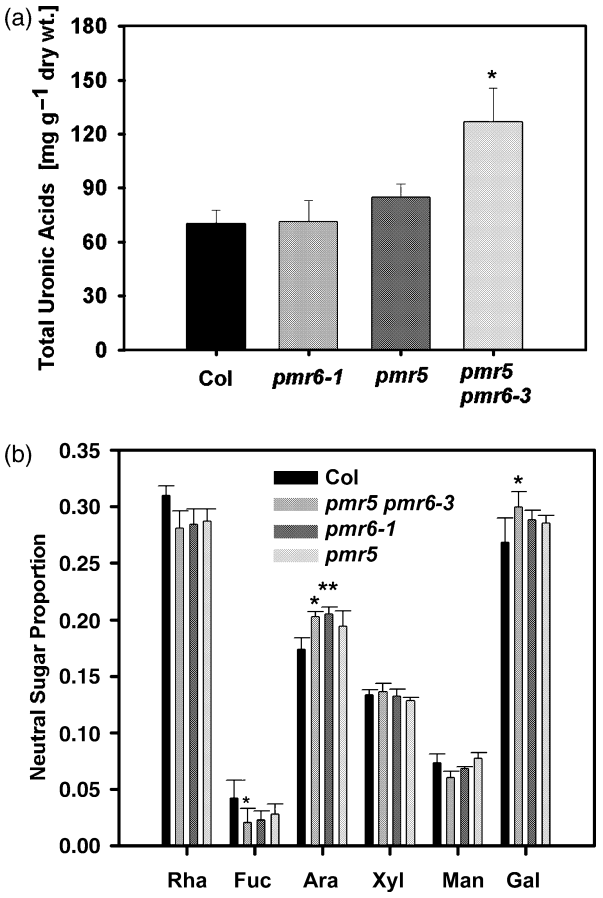

Figure 6. Sugar composition of *pmr* cell walls.
(a) Total uronic acid content. Mean ± SD based on rosette leaves from several plants ($n = 8$–12) are plotted. Bars marked with * were significantly ($P < 0.05$) different from Col based on a *t*-test.
(b) Neutral sugar profile of rosette leaves. Mean ± SD based on five to six plants are plotted. Bars marked with * ($P < 0.05$) or ** ($P < 0.01$) were significantly different from Col based on *t*-tests. Rha, rhamnose; Fuc, fucose; Ara, arabinose; Xyl, xylose; Man, mannose; Gal, galactose; Glc, glucose.

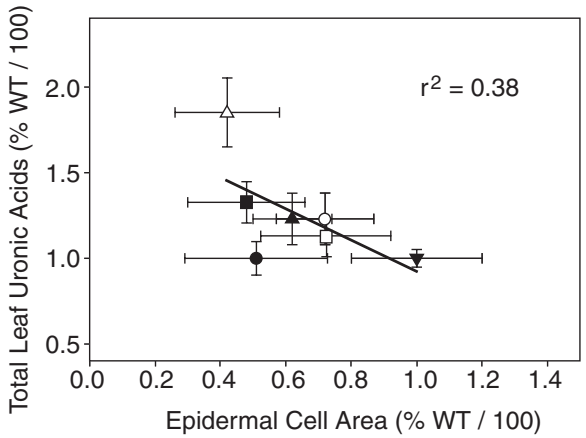

Figure 7. Relationship between cell size and pectin content.
Graph showing the relationship between total leaf uronic acid content and epidermal cell area. For epidermal cell area measurements, five to seven seedlings per genotype were fixed for microscopy, and four random fields selected on the adaxial surface of rapidly expanding rosette leaves for cell area determination. For uronic acid measurements, four to six leaves per genotype were analyzed. Line is the best-fit regression line through all seven genotypes.
Symbol legend: *Col-0*, ▼; *pmr 5* ■; *pmr 6*, ●; *pmr5 pmr6-3*, △; *CsLB2* SALK_21821, □; *bri1*-116, ○; *bri1 bzr1*, ▲.

absorption shoulder from 1730 to 1745 cm^{-1} in wild type and *pmr5* suggested that the degree of pectin methyl-esterification or *O*-acetylation was lower in *pmr5* cell walls (Fillipov, 1972; Synytsya *et al.*, 2003). Similar to *pmr6*, absorbance features from 1170 to 1050 cm^{-1} attributed to cellulose and xyloglucans were shifted down in energy, implying that either *pmr5* forms a different hydrogen bond network in its walls than wild type or the rigidity in cellulose-CH_2OH group rotation was changed (Figure 5a) (Vinogradov and Linell, 1971).

Principal component analysis was used to find more subtle differences between *pmr5* and wild-type spectra. The first and second principal components explained 56 and 15% of the variance in the original IR data set, respectively. The clearest separation of wild type and the *pmr5* mutant came from principal component 2 (Figure 5b). The second principal component had signals consistent with increased pectin and with decreased pectin esterification or *O*-acetylation in *pmr5* relative to wild-type cell walls (Figure 5d).

To determine whether *pmr5*, *pmr6*, or the *pmr5 pmr6-3* double mutant changed the proportion of monosaccharides contained in the polymers that make up the cell wall, we determined the concentration of sugars in acid-hydrolyzed cell walls. The acidic sugar galacturonic acid is of particular interest because it is a major component of pectin and is only found in pectin. As galacturonic acid is the dominant uronic acid found in cell walls, the other uronic acid is glucuronic acid, we used a simple spectrophotometric method to measure total uronic acids. This number should be directly proportional to the amount of pectin in the cell wall. *pmr5* cell walls exhibited an 18% increase in total uronic acids relative to wild type; however, this difference was not highly significant ($P = 0.056$). There was no increase in total leaf uronic acid content in *pmr6* leaves relative to wild-type leaves (Figure 6a). One possible explanation for why the total uronic acid content is unchanged in *pmr6* but the FTIR spectra suggest an increase in pectins is that the latter method measures only the outer epidermal cell wall composition. The *pmr5 pmr6-3* double mutant had higher levels of uronic acid than *pmr5* or *pmr6*, indicating that there was a synergistic interaction between the two mutations. Levels of neutral sugars in *pmr5* cell walls did not differ significantly from wild type (Figure 6b), while *pmr6* cell walls exhibited a modest but significant increase in arabinose. By contrast, the double mutant showed a statistically significant reduction in fucose and increases in arabinose

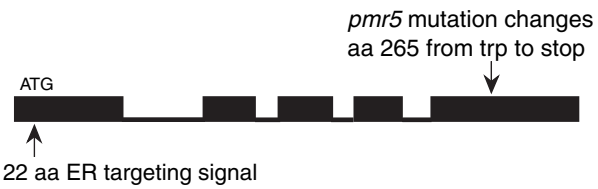

Figure 8. Structure of *PMR5*.
Exons are indicated by black boxes. The location of the endoplasmic reticulum (ER) targeting sequence and the mutation in *pmr5* are indicated by arrows. aa, amino acid.

and galactose relative to wild type. Collectively, these data reinforce the idea that the double mutant exhibits more dramatic cell wall changes than either of the single mutants.

Given the fact that pectin fills the space between adjacent plant cells and there is more pectin in the corners of the cell walls, the increased uronic acid content observed in the *pmr5 pmr6-3* double mutant could, in principle, be due to its smaller cell size rather than an alteration in pectin biosynthesis or degradation. To test this possibility, we determined the epidermal cell size and uronic acid content of Col, *pmr5*, *pmr6-1*, the *pmr5 pmr6-3* double mutant and of three dwarf mutants, *bri1-116*, a *bri1 bzr1* double mutant, and Salk insertion line 021821 (Figure 7). *bri1-116* carries a null allele of a brassinosteroid receptor kinase (Li and Chory, 1997), and *bzr1* a mutant allele of a transcriptional regulator of brassinosteroid sensing (Wang *et al.*, 2002). The insertion in Salk_021821 lies in a cellulose synthase-like gene, *CsLB2* (T.K. Raab and C.R. Somerville, unpublished data). Col and the mutants, *pmr5*, Salk_021821, *bri1* and *bri1 bzr1*, defined a weak inverse relationship between pectin content and epidermal cell size. However, *pmr6* and *pmr5 pmr6-3* did not fit this relationship, with *pmr6* showing reduced cell size but no increase in total leaf uronic acids and *pmr5 pmr6-3* having larger epidermal cells than predicted by the relationship defined by *pmr5* and Col. Thus, increases in total leaf uronic acids in the mutants cannot be attributed solely to a reduction in cell size.

Cloning PMR5

To better understand *pmr5*-mediated resistance, we cloned the corresponding gene using a positional cloning approach. Preliminary mapping using DNA from 22 F_2 plants placed *pmr5* between nga129 and LFY3 on the bottom of chromosome 5. To narrow this interval, several markers in the approximate position of *pmr5* were created. Two markers, JV57/58 on bacterial artificial chromosome (BAC) MUP24 and JV61/62 on BAC MDF20, were found to flank *pmr5*. Analysis of the entire mapping population of 901 F_2 plants with JV57/58 and JV61/62 identified 74 recombinants in the *pmr5* interval. These recombinants were then tested with markers in the JV57/58-JV61/62 interval to decrease the *pmr5*-containing interval. The minimum interval identified was 84 kbp as defined by markers JV94/95 on BAC MCK7 (one recombinant) and JV139/140 on BAC MZN1 (two recombinants).

Table 2 Gene expression pattern of *PMR5*

Tissue type[a]	No. replicates	Intensity[b]	SD
Flower-growth chamber[c]	2	5.66	1.47
Flower-greenhouse[c]	2	7.17	2.10
Leaf-growth chamber[c]	1	7.71	
Leaf-greenhouse[c]	2	4.96	0.81
Silique-greenhouse[c]	2	3.31	0.58
Stem-growth chamber[c]	2	2.46	0.03
Stem-greenhouse[c]	2	3.15	0.29
Leaf, uninoculated[d]	4	5.79	0.55
Leaf, 3 dpi with *E. cichoracearum*[d]	4	4.92	0.95

[a]All experiments were performed on Col, wild type.
[b]Average intensity values were divided by *ACT2/7* (Affymetrix ATH1 id: 250458_at_s) values and then multiplied by 100.
[c]Raw intensity values can be found at GenBank Series Accession GSE607 (http://www.ncbi.nlm.nih.gov/geo/) (Rhee *et al.*, 2003).
[d]Raw intensity values can be found at GenBank Series Accession GSE431 (Nishimura *et al.*, 2003).

The JV94/95-JV139/140 interval contained 40 genes or predicted genes. These candidate genes were subcloned into a binary vector and inserted into *pmr5* via *Agrobacterium*-mediated transformation. Two independent clones containing the same gene, locus AT5G58600, restored powdery mildew susceptibility and wild-type stature to *pmr5* in 104 of the 107 T1 plants examined (Figure 3). Thus, *PMR5* must be AT5G58600. To further verify that we had cloned the correct gene, the *PMR5* region from *pmr5* mutant plants was sequenced to determine the specific mutation. A single base change, G–A, that changes a trp codon (TGG) encoding amino acid 265 to a stop codon (TGA) was identified (Figure 8).

A BLAST search with genomic *PMR5* sequence identified six previously reported cDNA clones. The longest clone (GenBank AK117382) was 1398 bases long. The *PMR5* open reading frame is predicted to encode a 402-aa protein with a mass of 44.8 kDa. A comparison of the mRNA sequence to the genomic sequence revealed that *PMR5* contains four introns (Figure 8). A BLAST search with the predicted protein sequence revealed that PMR5 belongs to a large family of plant-specific genes of unknown function, with 45 members in Arabidopsis. The first 22 aa of PMR5 are predicted to serve as a non-cleavable signal sequence that targets the protein to the endoplasmic reticulum (Target P: Olof *et al.*, 2000; PSORT: Nakai and Horton, 1999; ProtFun 1.1: Jensen *et al.*, 2002).

Microarray analysis showed that *PMR5* was expressed at approximately the same level in all tissues tested; flowers, siliques, stems, uninfected leaves and leaves 3 dpi with *Erysiphe cichoracearum* (Table 2) (Nishimura *et al.*, 2003; Rhee *et al.*, 2003).

Discussion

As in the *pmr6* mutants, three lines of evidence indicate that the resistance mechanism operating in the *pmr5* mutant does not require the activation of either the SA or JA/ethylene defense pathways. First, *pmr5* plants did not constitutively express high levels of either *PR1* or *PDF1.2* mRNA indicating that resistance is not mediated by constitutive activation of the SA or JA/ethylene pathways. Secondly, neither *PR1* nor *PDF1.2* was induced to high levels after inoculation indicating that the resistance is not mediated by a hyperactivation of either of these signal transduction pathways. Thirdly, and most convincingly, mutants or transgenes that block signaling through the SA or JA/ethylene pathways did not abolish powdery mildew resistance in *pmr5* plants. Thus, *pmr5*-mediated resistance is independent of the activation of known defense pathways. Therefore, PMR5 is either required for fungal growth or the *pmr5* mutation activates a novel defense pathway.

Unlike resistance attributed to the majority of resistance genes and disease-resistant mutants, the attenuation of powdery mildew growth on *pmr5* and *pmr6* did not require cell death as shown by the lack of cell death below fungal colonies. In the course of looking for resistance-associated cell death, we noticed that both *pmr5* and *pmr6* had microlesions along veins on a subset of the oldest leaves. This phenotype was not correlated with resistance because only a small subset of the oldest leaves had lesions, yet all leaves were highly resistant. We previously showed that this phenotype can be phenocopied by heat treatment of wild-type plants (Vogel *et al.*, 2002). Importantly, heat-treated plants were still susceptible to powdery mildew. We view the microlesions as a pleiotropic effect of the *pmr5* and *pmr6* mutations unrelated to disease resistance. These microlesions may be responsible for the slightly elevated basal level of *PR1* observed in *pmr5* and *pmr6*. That both *pmr5* and *pmr6* have these microlesions underscores the similarity of these mutants.

As both *pmr5* and *pmr6* were fully susceptible to *P. syringae* pv tomato and *P. parasitica*, the resistance is not due to the activation of a broad-spectrum defense pathway, like systemic acquired resistance. Both *pmr5* and *pmr6* were resistant to *E. orontii* indicating that the resistance is effective against isolates from two powdery mildew species. Thus, *pmr5* and *pmr6* resistance is qualitatively different than resistance conferred by either gene-for-gene resistance genes or previously described disease-resistant mutants.

The FTIR spectra from *pmr5* epidermal cell walls were similar to the spectra from *pmr6* suggesting that both mutants have increased pectin and the pectin had lower methyl esterification or *O*-acetylation relative to wild type. Moreover, like *pmr6*, the major FTIR spectral features associated with cellulose and xyloglucan shifted in energy in *pmr5* cell walls, suggesting an alteration in the hydrogen-bonding environment. Interestingly, the *pmr5 pmr6-3* double mutant had higher levels of uronic acid than either *pmr5* or *prm6* indicating that these two mutants interact synergistically to increase uronic acid content. The synergistic effect on uronic acid content along with the similarity of *pmr5* and *pmr6* phenotypes (e.g. powdery mildew resistance, morphology, microlesions, cell wall composition) suggests that these two mutations affect parallel pathways that regulate some aspects of pectin biosynthesis either directly or indirectly. Furthermore, PMR5 is predicted to be associated with the endoplasmic reticulum by a hydrophobic N-terminal signal sequence and PMR6 is predicted to locate to the exterior side of the plasma membrane via a glycosylphosphatidylinositol anchor. Thus, it is unlikely that these two proteins interact directly.

To address the possibility that the increase in uronic acid observed in the *pmr5 pmr6-3* double mutant was due to an indirect effect of cell size, we determined the relationship between cell size and pectin content in three dwarf mutants that were not directly related to disease resistance or pectin metabolism. Our results indicated that, while the wild type, the three dwarfs and *pmr5* did show a weak correlation between cell size and pectin content, the large increase in uronic acid observed for the *pmr5 pmr6-3* double mutant could not be attributed solely to decreased cell size. Thus, it is possible that the increase in pectin in *pmr5 pmr6-3* cell walls restricts cell expansion and this in turn limits cell size.

The cell wall is very dynamic and responds to physiological stresses and altered substrate availability with compensating changes in organization (Gillmor *et al.*, 2002). To assess whether the changes in pectin content inferred from the FTIR spectra were associated with any compensating changes in other components, we measured the cell wall neutral sugar content. Aside from the approximately 50% reduction in fucose in the double mutant, all other statistically significant changes in neutral sugars were modest. As approximately two-thirds of the fucose in the Arabidopsis leaf cell wall is found in xyloglucan, the decreased fucose in the double mutant may suggest decreased xyloglucan fucosylation (Perrin *et al.*, 2003; Zablackis *et al.*, 1995). The presence of relatively normal amounts of xylose in the double mutant suggests that the amount of xyloglucan is not strongly altered. *pmr5 pmr6-3* cell walls had small but significant increases in arabinose and galactose suggesting increased abundance of the galactose and arabinose-containing side chains of the pectin, rhamnogalacturonan I.

Our characterization of *pmr5* revealed that *pmr5*-mediated resistance does not require the activation of the SA or JA/ethylene defense pathways, does not require cell death, and is not broad-spectrum. In addition, the phenotype of *pmr5* plants is very similar to *pmr6* plants. Taken together, these data suggest that *pmr5* and *pmr6* employ similar

mechanisms to limit fungal growth and that this mechanism is unrelated to known defense signaling pathways. There are several possible explanations for the disease resistance of the *pmr5* mutant. This mutant may be a less hospitable host for powdery mildews. For example, the *pmr5* extrahaustorial matrix may have altered composition, especially of modified pectins, decreasing nutrient transport to the fungus or the powdery mildew pathogen may have limited ability to digest the *pmr5* outer epidermal cell wall. Alternatively, the *pmr5* cell wall may carry latent signaling molecules that are released upon powdery mildew infections to activate novel defenses (Vorwerk *et al.*, 2004). Whatever the basis for disease resistance, the *pmr5* and *pmr6* mutants highlight the importance of cell wall composition in plant–pathogen interactions.

Experimental procedures

Growth conditions, pathogen inoculations, and microscopy

Plants were grown and pathogen inoculations were performed as previously described (Vogel and Somerville, 2000; Vogel *et al.*, 2002). All staining, microscopy and cell size determinations were as previously described (Vogel and Somerville, 2000; Vogel *et al.*, 2002). Epidermal cell areas given in Figure 7 were measured as follows: leaves from 18-day-old Col-0, *pmr5*, *pmr6-3*, *bri1-116* (Li and Chory, 1997), SALK _021821, *pmr5 pmr6-3*, and *bri1 bzr1* plants (Wang *et al.*, 2002) were cleared in 3:1 (v/v) ethanol:acetic acid, and rehydrated through a series of 70% ethanol, 35% ethanol and 17% ethanol. Leaf tissues were equilibrated and mounted in Hoyer's solution and then visualized with DIC on a Nikon E600 microscope (Nikon Instruments, Melville, NY, USA) at 40× (Gillmor *et al.*, 2002). Digital pictures were captured using a SPOT CCD camera. Epidermal cells were outlined using automatic edge detection and the areas calculated using ImageJ 1.22 software (NIH website: http://rsb.info.nih.gov/ij/).

Double mutant construction

Prior to characterization, including double mutant construction, *pmr5* was backcrossed to Col twice. The *pmr5 ein2-1* double mutant was created by crossing *pmr5* with *ein2-1* (Alonso *et al.*, 1999). To identify plants homozygous for the *ein2-1* mutation, F_2 seeds were plated on Murashige and Skoog medium supplemented with 10 μM 1-aminocyclopropane-1-carboxylic acid (ethylene-insensitive plants are tall in the presence of this compound). Several ethylene-insensitive plants were transferred to soil, grown for 2 weeks, and inoculated with powdery mildew to identify plants homozygous for *pmr5*. The *pmr5 npr1-1* and *pmr5 coi1* double mutants were constructed as described for *pmr6* (Vogel *et al.*, 2002). Likewise, the *NahG* transgene was crossed into the *pmr5* background as described for *pmr6*.

The *pmr5 pmr6-3* double mutant was constructed by crossing *pmr5* with *pmr6-3* (Vogel *et al.*, 2002). The double mutant was identified using the following strategy: first, powdery mildew-resistant F_2 plants were selected. These plants were homozygous for *pmr5* and/or *pmr6-3*. These plants were then treated with Finale herbicide (0.13% active ingredient) (AgrEvo, Berlin, Germany) to identify plants either homozygous or heterozygous for *pmr6-3*. Finale-resistant plants were allowed to set seed. The resulting F_3 families were then planted and treated with Finale to identify a family that segregated 3:1 for Finale resistance. This family must have come from an F_2 individual that was homozygous for *pmr5* and heterozygous for *pmr6-3*. Finale-resistant F_3 plants from this family were selected and allowed to set seed. F_4 families were then treated with Finale to identify a family homozygous for Finale resistance and, by inference, *pmr6-3*. A single F_4 plant was chosen as the *pmr5 pmr6-3* double mutant and allowed to set seed that was used for all experiments involving the *pmr5 pmr6-3* double mutant. To confirm the double mutant, the selected F_4 plant was test crossed to *pmr5* and *pmr6-3* (data not shown).

Fourier transform infrared analysis

Leaf disks from 12 Col plants and 14 *pmr5* plants, dark-adapted overnight to deplete diurnal starch reserves, were extracted with 1:1 (v/v) chloroform:MeOH to remove lipids (Vogel *et al.*, 2002) and analyzed in reflection mode on an IR microscope at Beamline 1.4.3 at Lawrence Berkeley Lab's Advanced Light Source synchrotron (Raab and Martin, 2001). Spectra were collected and analyzed as described (Vogel *et al.*, 2002) with the exception that 256 scans were co-added in this study.

Sugar analysis

Individual leaf disks previously used for the FTIR analysis were dried, weighed, and acid-hydrolyzed (Reiter *et al.*, 1997). Neutral sugars were quantified by separation of their partially methylated alditol acetate derivatives essentially as described in Reiter *et al.* (1997). Myoinositol (Sigma-Aldrich, St Louis, MO, USA) was added as an internal standard. An aliquot of each acid hydrolysate was used for total uronic acid determination (Blumenkrantz and Asboe-Hansen, 1973). Pure galacturonic acid (Sigma-Aldrich) was used as a standard.

Cloning PMR5

A map-based cloning approach was used to identify *PMR5*. DNA was extracted from 901 powdery mildew-resistant F_2 plants from a *pmr5* (Col background) × wild type (WS background) cross (Klimyuk *et al.*, 1993). A subset of this population was used for the initial rough mapping. Once a rough map position was determined, markers were created by scanning BAC sequences in the interval for simple sequence repeats and designing flanking oligonucleotide primers to test for polymorphisms between Col and WS. Markers were also created by sequencing predicted intergenic regions to identify single nucleotide polymorphisms. Details of the markers generated in this study can be found on the TAIR website (http://www.arabidopsis.org).

Genes in the interval containing *pmr5* were subcloned into the binary transformation vector pCAMBIA3300 (CAMBIA, Canberra, Australia) either by subcloning BAC DNA or by amplifying individual genes using PCR. PCR-amplified DNA fragments were cloned into pGEM-T prior to subcloning into pCAMBIA3300 using an *Xma*I site contained in the primer sequence. Transformants were selected on soil using Finale. T_1 transformants were challenged with *E. cichoracearum*. The two independent plasmids (pC32A1 and pC32B1) that complemented the *pmr5* mutation were created by amplifying the *PMR5* interval, including 709 bases 5′ of the start codon and 1070 bases 3′ of the poly A signal, using the following primers: JV192 (5′-acccgggaaagggacccgcttagtcat) and JV193 (5′-acccgggtcacgaagaaggtcaaaatgc).

Acknowledgements

We thank Jennifer Milne, Marc Nishimura, Sue Thayer, and Heather Youngs for their valuable comments and we thank the Carnegie Institution of Washington, the IRM Ltd and the U.S. Department of Energy for financial support. J. Vogel was supported in part by an NIH postdoctoral fellowship. The Advanced Light Source is supported by the Director, Office of Science, Office of Basic Energy Sciences, Materials Sciences Division, of the U.S. Department of Energy under contract no. DE-AC03-76SF00098 at Lawrence Berkeley National Laboratory.

References

Alonso, J.M., Hirayama, T., Roman, G., Nourizadeh, S. and Ecker, J.R. (1999) *Ein2*, a bifunctional transducer of ethylene and stress responses in Arabidopsis. *Science*, **284**, 2148–2152.

Blumenkrantz, N. and Asboe-Hansen, G. (1973) New method for quantitative determination of uronic acids. *Anal. Biochem.* **54**, 484–489.

Cao, H., Bowling, S.A., Gordon, A.S. and Dong, X.N. (1994) Characterization of an Arabidopsis mutant that is nonresponsive to inducers of systemic acquired-resistance. *Plant Cell*, **6**, 1583–1592.

Coimbra, M.A., Barros, A., Barros, M., Rutledge, D.N. and Delgadillio, I. (1998) Multivariate analysis of uronic acid and neutral sugars in whole pectic samples by FT-IR spectroscopy. *Carbohydr. Polym.* **37**, 241–248.

Dangl, J.L., Ritter, C., Gibbon, M.J., Mur, L.A., Wood, J.R., Goss, S., Mansfield, J., Taylor, J.D. and Vivian, A. (1992) Functional homologs of the Arabidopsis *rpm1* disease resistance gene in bean and pea. *Plant Cell*, **4**, 1359–1369.

Fillipov, M.P. (1972) IR spectra of pectin films. *J. Appl. Spectrosc.* **17**, 1052–1054.

Gillmor, C.S., Poindexter, P., Lorieau, J., Sujino, K., Palcic, M. and Somerville, C.R. (2002) The α-glucosidase I encoded by the KNOPF gene is required for cellulose biosynthesis and embryo morphogenesis in Arabidopsis. *J. Cell Biol.* **256**, 1003–1013.

Glazebrook, J. (2001) Genes controlling expression of defense responses in Arabidopsis – 2001 status. *Curr. Opin. Plant Biol.* **4**, 301–308.

Jensen, L.J., Gupta, R., Blom, N. *et al.* (2002) Prediction of human protein function from post-translational modifications and localization features. *J. Mol. Biol.* **319**, 1257–1265.

Kacurakova, M., Capek, P., Sasinkova, V., Wellner, N. and Ebringerova, A. (2000) FT-IR study of plant cell wall model compounds: pectic polysaccharides and hemicelluloses. *Carbohydr. Polym.* **43**, 195–203.

Klimyuk, V.I., Carroll, B.J., Thomas, C.M. and Jones, J.D.G. (1993) Alkali treatment for rapid preparation of plant material for reliable PCR analysis. *Plant J.* **3**, 493–494.

Lawton, K., Weymann, K., Friedrich, L., Vernooij, B., Uknes, S. and Ryals, J. (1995) Systemic acquired resistance in Arabidopsis requires salicylic acid but not ethylene. *Mol. Plant Microbe Interact.* **8**, 863–870.

Li, J. and Chory, J. (1997) A putative leucine-rich repeat receptor kinase involved in brassinosteroid signal transduction. *Cell*, **90**, 929–938.

Nakai, K. and Horton, P. (1999) PSORT: a program for detecting sorting signals in proteins and predicting their subcellular localization. *Trends Biochem. Sci.* **24**, 34–36.

Nishimura, M., Stein, M., Hou, B.-H., Vogel, J.P., Edwards, H. and Somerville, S.C. (2003) Loss of a callose synthase results in salicylic acid-dependent disease resistance. *Science*, **301**, 969–972.

Olof, E., Nielsen, H., Brunak, S. and Heijne, G. (2000) Predicting subcellular localization of proteins based on their N-terminal amino acid sequence. *J. Mol. Biol.* **300**, 1005–1016.

Panstruga, R. (2003) Establishing compatibility between plants and obligate biotrophic pathogens. *Curr. Opin. Plant Biol.* **6**, 320–326.

Pelton, J.T. and McLean, L.R. (2000) Spectroscopic methods for analysis of protein secondary structure. *Anal. Biochem.* **277**, 167–176.

Penninckx, I., Eggermont, K., Terras, F.R.G., Thomma, B., Desamblanx, G.W., Buchala, A., Metraux, J.P., Manners, J.M. and Broekaert, W.F. (1996) Pathogen-induced systemic activation of a plant defensin gene in Arabidopsis follows a salicylic acid-independent pathway. *Plant Cell*, **8**, 2309–2323.

Perrin, R.M., Jia, X., Wagner, T.A., O'Neill, M.A., Sarria, R., York, W.S., Raikhel, N.V. and Keegstra, K. (2003) Analysis of xyloglucan fucosylation in Arabidopsis. *Plant Physiol.* **132**, 768–778.

Plotnikova, J.M., Reuber, T.L. and Ausubel, F.M. (1998) Powdery mildew pathogenesis of *Arabidopsis thaliana*. *Mycologia*, **90**, 1009–1016.

Raab, T.K. and Martin, M.C. (2001) Visualizing the rhizosphere chemistry of legumes with midinfrared synchrotron radiation. *Planta*, **213**, 881–887.

Reiter, W.D., Chapple, C. and Somerville, C.R. (1997) Mutants of *Arabidopsis thaliana* with altered cell wall polysaccharide composition. *Plant J.* **12**, 335–345.

Rhee, S.Y., Osborne, E., Poindexter, P.D. and Somerville, C.R. (2003) Microspore separation in the *quartet 3* mutants of Arabidopsis is impaired by a defect in a developmentally regulated polygalacturonase required for pollen mother cell wall degradation. *Plant Physiol.* **133**, 1170–1180.

Schulze-Lefert, P. and Vogel, J. (2000) Closing the ranks to attack by powdery mildew. *Trends Plant Sci.* **5**, 343–347.

Synytsya, A., Copikova, J., Matejka, P. and Machovic, V. (2003) Fourier transform Raman and infrared spectroscopy of pectins. *Carbohydr. Polym.* **54**, 97–106.

Vincken, J.-P., Schols, H.A., Oomen, R.J.F.J., McCann, M.C., Ulvskov, P., Voragen, A.G.J. and Visser, R.G.F. (2003) If homogalacturonan were a side chain of rhamnogalacturonan I. Implications for cell wall architecture. *Plant Physiol.* **132**, 1781–1789.

Vinogradov, S. and Linell, R.H. (1971) *Hydrogen Bonding*. New York: Van Nostrand Reinhold.

Vogel, J. and Somerville, S. (2000) Isolation and characterization of powdery mildew-resistant Arabidopsis mutants. *Proc. Natl Acad. Sci. USA*, **97**, 1897–1902.

Vogel, J.P., Raab, T.K., Schiff, C. and Somerville, S.C. (2002) *PMR6*, a pectate lyase-like gene required for powdery mildew susceptibility in Arabidopsis. *Plant Cell*, **14**, 2095–2106.

Vorwerk, S., Somerville, S. and Somerville, C. (2004) The role of plant cell wall polysaccharide composition in disease resistance. *Trends Plant Sci.* **9**, 203–209.

Wang, Z.-Y., Nakano, T., Gendron, J. *et al.* (2002) Nuclear-localized BZR1 mediates brassinosteroid-induced growth and feedback suppression of brassinosteroid biosynthesis. *Dev. Cell*, **2**, 1–20.

Wellner, N., Kacurakova, M., Malovikova, A., Wilson, R.H. and Belton, P.S. (1998) FT-IR study of pectate and pectinate gels formed by divalent cations. *Carbohydr. Res.* **308**, 123–131.

Whalen, M.C., Innes, R.W., Bent, A.F. and Staskawicz, B.J. (1991) Identification of *Pseudomonas syringae* pathogens of Arabidopsis and a bacterial locus determining avirulence on both Arabidopsis and soybean. *Plant Cell*, **3**, 49–59.

Wilson, R.H., Smith, A.C., Kacurakova, M., Saunders, P.K., Wellner, N. and Waldron, K.W. (2000) The mechanical properties and molecular dynamics of plant cell wall polysaccharides studied by

Fourier-transform infrared spectroscopy. *Plant Physiol.* **124**, 397–405.

Xie, D.X., Feys, B.F., James, S., NietoRostro, M. and Turner, J.G. (1998) *COI1*: an Arabidopsis gene required for jasmonate-regulated defense and fertility. *Science*, **280**, 1091–1094.

Zablackis, E., Huang, J., Muller, B., Darvill, A.G. and Albersheim, P. (1995) Characterization of the cell wall polysaccharides of *Arabidopsis thaliana* leaves. *Plant Physiol.* **107**, 1129–1138.

Accession numbers: *pmr5*, *pmr6-3*, and *pmr5 pmr6-3* will be submitted to the Arabidopsis Biological Resource Center upon publication. *PMR5* corresponds to AT5G58600.